Arabian Journal of Chemistry (2020) 13, 6274–6284

King Saud University

Arabian Journal of Chemistry

www.ksu.edu.sa
www.sciencedirect.com

ORIGINAL ARTICLE

Synergistic effect of graphene oxide and boron-nitrogen structure on flame retardancy of natural rubber/IFR composites

Na Wang [a,b,c,*], Hao Liu [a], Jing Zhang [a], Miao Zhang [a], Qinghong Fang [a,b], Deyi Wang [d,*]

[a] Sino-Spanish Advanced Materials Institute, Shenyang University of Chemical Technology, Shenyang 110142, China
[b] Liaoning Provincial Key Laboratory of Rubber & Elastomer, Shenyang 110142, China
[c] Key Laboratory on Resources Chemicals and Material of Ministry of Education, Shenyang University Chemical Technology, Shenyang 110142, China
[d] IMDEA Materials Institute, C/Eric Kandel, 2, 28906 Getafe, Madrid, Spain

Received 14 March 2020; accepted 9 May 2020
Available online 1 June 2020

KEYWORDS

Natural rubber;
Flame retardant;
Graphene oxide;
Boron nitride

Abstract In this paper, GO-BN(graphene oxide grafted boron nitride) was synthesized from graphene oxide and boron nitride by silane coupling agent KH550. Furthermore, GO-BN and intumescent flame retardant (IFR) were added into natural rubber (NR) simultaneously to improve its flame retardancy. The structure of GO-BN was studied by Fourier transform infrared spectroscopy (FTIR) and X-ray photoelectron spectroscopy (XPS). The analysis showed that GO-BN was successfully synthesized. The enhanced flame retardancy performance of flame retardant natural rubber (FRNR) was evaluated by limiting oxygen index (LOI) and UL-94 tests. Moreover, the combustion action of FRNR in fire was evaluated by cone calorimetry. Notably, the results showed that the sample with a GO-BN content of 12 phr showed the best flame retardancy performance. The heat release rate (HRR) and total heat release rate (THR) were remarkably decreased by 42.8% and 19.4%, respectively. Carbon residues were analyzed by infrared spectroscopy and scanning electron microscopy, which showed that GO-BN and IFR had a synergistic catalytic effect.

* Corresponding authors at: Sino-Spanish Advanced Materials Institute, Shenyang University of Chemical Technology, Shenyang 110142, China (N. Wang); IMDEA Materials Institute, C/Eric Kandel, 2, 28906 Getafe, Madrid, Spain (D. Wang).
E-mail addresses: iamwangna@syuct.edu.cn (N. Wang), liuh1104@163.com (H. Liu), zhangjingcszx@syuct.edu.cn (J. Zhang), iamzhangmiao@163.com (M. Zhang), qinghongfang@syuct.edu.cn (Q. Fang), deyi.wang@imdea.org (D. Wang).
Peer review under responsibility of King Saud University.

ELSEVIER Production and hosting by Elsevier

https://doi.org/10.1016/j.arabjc.2020.05.016

The formation of compact thermal stable carbon layer after combustion was the key to protect engineering materials from combustion.

1. Introduction

Natural rubber (NR) is an important type of polymer, which is widely used in our daily lives and also in industrial applications (Carli et al., 2011). It is the most widely used general rubber due to its excellent mechanical properties and very high chemical resistance. It is employed in the manufacture of conveyor belts, cables, tires, and so on (Wang et al., 2009). However, due to its molecular structure, it is classified as a flammable material. Its limiting oxygen index (LOI) is only 18%, which limits its application (Wang et al., 2013; Wang et al., 2016). Therefore, several methods have been explored to improve its flame retardancy. One of the most effective ways to enhance the flame retardancy of natural rubber is through the addition of flame retardants (Wang et al., 2018; Wang et al., 2017; Wang et al., 2014).

The commonly used flame retardants include intumescent flame retardants, halogen-containing flame retardants, inorganic flame retardants, and organic flame retardants (Fang et al., 2008; Rabe et al., 2017; Xue et al., 2017; Wang et al., 2018; Rabe and Chuenban, 2017). The intumescent flame retardant system consists of an acid source, carbon source and gas source (Iqbal et al., 2016; Alongi et al., 2015; Cui and Qu, 2010; Qin et al., 2016). It has the advantages of low smoke, low toxicity, and no dripping. But in comparison with other flame retardants, it has the disadvantages of poor dispersion in composite materials and also needs to add in large amounts. Consequently, researchers have found that the addition of synergists in combination with flame retardants in polymer composites can not only significantly improve the flame retardancy of composites, but also reduce the amount of flame retardants (Yan et al., 2019; Tang et al., 2003; Yang and Yang, 2005).

In recent years, Graphene oxide has attracted a huge interest across different research areas. It is composed of carbon atoms with a two-dimensional crystal structure and only one atom layer (Fan et al., 2019; Qiu et al., 2015; Zhang et al., 2017; Wang et al., 2016; Chen et al., 2019). It was reported that graphene oxide as a synergistic flame retardant, produces a huge insulating layer in the combustion process of the composite, which can increase the carbon residue of the composite and improve the flame retardancy of the composite (Vahabi et al., 2018; Vahabi et al., 2018; Feng et al., 2020; Feng et al., 2019; Feng et al., 2018). In the previous work of our group, we prepared intumescent flame retardant materials with modified graphene oxide as synergist. We modified graphene oxide with nano-mesoporous molecular sieves and benzoic acid, and applied it in composite materials to improve their flame retardancy (Wang et al., 2018; Zhang et al., 2017). It was also found that functionalized graphene can inhibit the regeneration of original graphite and reduce the occurrence of agglomeration. The rubber and thermosetting resin materials with the addition of functional graphene have a good influence on the curing process and improve the mechanical properties of the materials (Yu et al., 2015). Moreover, we found that hexagonal boron nitride with graphene oxide-like structure, has itself has good mechanical properties and on the premise of good compatibility, the addition of a small amount of boron nitride can greatly improve the mechanical properties of polymers (Wang et al., 2018; Zhoong et al., 2015; Das et al., 2010; Das and Ghatak, 2012; Kahraman et al., 2019; Sasan et al., 2019; Stengl et al., 2014). It can obviously improve the comprehensive properties of polymer materials. Therefore, a new type of flame retardant and enhanced synergist GO-BN has been studied in our laboratory.

In this study, the synergistic mechanism of GO-BN in FRNR is investigated. The structure of GO-BN was characterized by Fourier transform infrared spectroscopy (FTIR) and X-ray photoelectron spectroscopy (XPS). The effects of GO-BN on flame retardancy, charring property and thermal decomposition behavior of natural rubber were also investigated. The importance of thermally stable and compact carbon residue in flame retardant natural rubber system was explained by the corresponding mechanism study.

2. Materials and methods

2.1. Materials

The graphite powder was supplied by Beijing Deke Graphite Co., Ltd., Beijing, China. KH-550 was purchased from Shandong Yousuo Chemical Co., Ltd. BN was provided by Shanghai Aladdin Biochemical Technology Co., Ltd. Sulfuric acid (H_2SO_4, 98%), potassium permanganate ($KMnO_4$), ammonia (25–28% aq), hydrogen peroxide (H_2O_2, 30% aq), were used as received and Hydrochloric acid (HCl, 37% aq, diluted to 5 wt% before use). NR SMR-20 was provided by Hainan state farms Group Co., Ltd., Haikou, China. 1-Ethyl-3-(3-dimethylaminopropyl) carbodiimide(EDC)was purchased from Shandong West Asia Chemical Industry Co., Ltd. N-hydroxysuccinimide(NHS)was provided by Sinopharm Chemical Reagent Co., Ltd. The commercial product APP (phase II, average degree of polymerization $n > 1000$, soluble in $H_2O < 0.5$ mass %) was bought from Shifang Changfeng Chemical Co., Ltd., Chengdu, China. PER and MEL were supplied by Sinopharm Chemical Reagent Co., Ltd., Shenyang, China. The mass ratio of APP, PER, and MEL in the IFR mixture was 3:1:1. Carbon black and age inhibitor 4010 were bought from Sheng Ao Chemical Co., Ltd., Tianjin, China. Analytical grade ZnO was provided by Dalian ZnO factory, Dalian, China. Accelerant CZ and tetramethyl thiuram disulfide were purchased from Tianjin No.1 Organic Chemical Plant, Tianjin, China. Sulfur was purchased from Tong Chuang Chemical Co., Ltd., Taizhou, China.

2.2. Methods

2.2.1. Preparation of GO

GO was obtained from natural graphite by a modified Hummers method (Guo et al., 2011). Weighing 1.4 g of graphite powder and pouring it into a three-necked flask, then 2.4 g of $NaNO_3$ powder and 87.5 ml of H_2SO_4 are added into the flask, and stirring it for 40 min under the ice bath condition by mechanical agitation, which the stir speed of 300 rpm/min. After that, weighing 7.5 g of $KMnO_4$, dividing $KMnO_4$ into smaller portions and adding them all to the three-necked flask within an hour (to prevent an accident as a result of the violent reaction), stirring for 2 h under the ice bath condition after adding, which the stir speed of 550 rpm/min. Then increase the temperature to 40 °C and continue to stir for 40 min, which the stir speed is 200 rpm/min. Taking 250 ml of deionized water, add it into the three-necked flask by a burette. After all the deionized water has been added, increase the temperature of the system to 98 °C and stir for 15 min, which the stir speed is 500 rpm/min. Pouring the mixture into 400 ml of deionized water and stir well. The next step is to add H_2O_2 drop by drop until the solution turns golden, and let stand for 12 h. When the completion of standing, use centrifugal washing with 1% HCl for three times. Centrifugal wash with the deionized water three times and dry for later use.

2.2.2. Preparation of modified BN

Firstly, 10 g BN powder was weighed and transferred into a 500 ml three-neck bottle, then 150 ml of 5 M NaOH solution was added. The solution was heated and stirred for 18 h at 98 °C, so that more hydroxide ions can be adsorbed on the surface of BN. The solution was then dried and rinsed repeatedly with water until the pH value was adjusted to neutral. It was then dried for 5 h at 90 °C in the oven. Afterward it was cooled to room temperature, take out sealed storage and hydroxylated BN powder was obtained. Secondly, we added 7 ml of distilled water, 1 ml of 10 M H_2SO_4 solution, 2 ml of glycerol, 10 ml of methanol and 80 ml of ethanol successively into the flask with three necks. After homogeneous mixing, 5 ml of KH550 was added, and the hydrolysis was completed by stirring for 30 min at 50 °C. Finally, the hydroxylated BN was added to the above solution and stirred for 3 h at 70 °C. Then, the resulting product was washed repeatedly with ethanol and distilled water to a neutral pH. The product was dried in a vacuum oven for more than 8 h at 90 °C. The final product was cooled to room temperature, sealed and marked as BN-KH550 products.

2.2.3. Preparation of GO-BN

A scheme for the synthesis of GO-BN is shown in Fig. 1. Firstly, to prepare activated graphene oxide. EDC was dissolved in distilled water, and the pH of graphene solution was adjusted to 4–6 with dilute hydrochloric acid. Afterward the dissolved EDC was added to the graphene solution. Then the pH value was set to 7–8, followed by the addition of NHS. Finally, the BN-KH550 powder (10 g) was weighed and added to the activated graphene oxide (10 g) solution. The ultrasonic vibration lasted for 30 min. Then the undissolved BN powder was centrifuged for 5 min with 3000 r/min. Remove the underlying solids and dry them for later use.

2.2.4. Preparation of FRNR composites

Different compositions of FRNR composites were prepared by mixing IFR agents with NR via the two-roll milling method. The compositions of FRNR composites are listed in Table 1. The fixed values of carbon black, zinc oxide, stearic acid, sulfur, age inhibitor 4010, accelerant CZ, electric insulating oil, and tetramethyl thiuram disulfide were 35 g, 5 g, 5 g, 4 g, 1.2 g, 1 g, 1 g, 0.8 g and 0.35 g . All samples were vulcanized at a temperature of 145 °C and at a certain pressure. The optimum cure time t_{90} was determined by a GT-M2000-A rheometer (GaoTie Limited Co., Taiwan). All specimens were cut into vulcanized sheets at room temperature for 24 h before subsequent use.

2.2.5. Instrumental

The Fourier transform infrared spectra of samples were measured with a Nicolet MAGNA-IR 560 with 4 cm^{-1} resolution. The vulcanization curve of raw rubber was tested by GT-M2000-A rubber vulcanization tester produced by High-

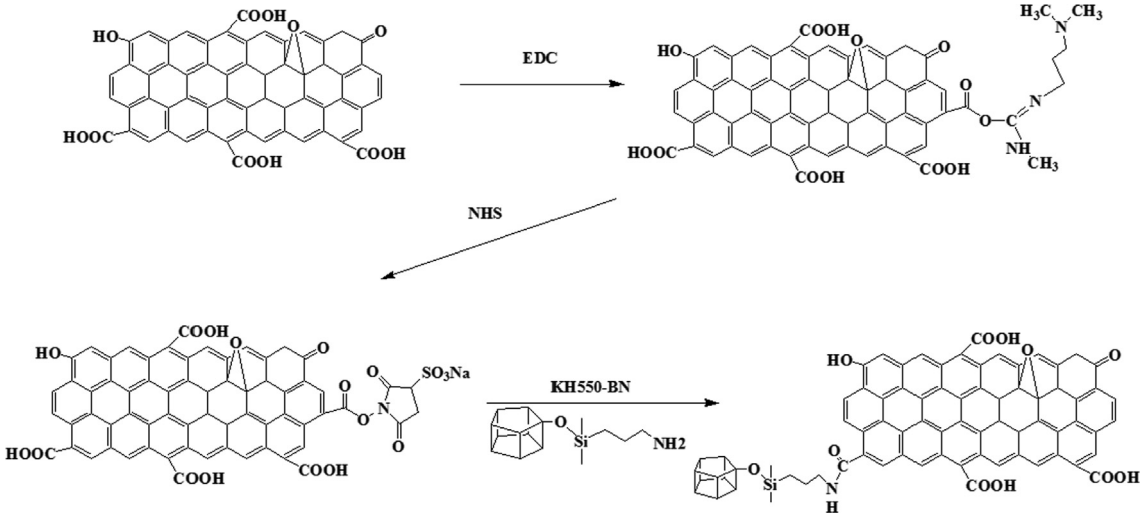

Fig. 1 Reaction process of GO-BN.

Table 1 Composition of NR composites.

Samples	NR/phr	IFR/phr	GO-BN/phr
NR1	150	0	0
NR2	100	50	0
NR3	100	46	4
NR4	100	42	8
NR5	100	38	12
NR6	100	34	16

speed Rail Testing Instrument Co., Ltd. According to GB/T 10707–2008 standard, the limit oxygen index (LOI) data were measured at room temperature by JF-3 oxygen index instrument provided by Jiangning Analytical Instrument Co., Ltd. CZF-3 instrument was used to test the vertical combustion test (UL-94 test). The sample sizes were 150 mm × 6.5 mm × 3 mm and (126 ± 3) mm × (13.0 ± 0.3) mm × (3.0 ± 0.2) mm, respectively. All samples were tested five times. Room temperature tensile tests were measured on an Instron 1211 testing machine, GaoTie Limited Co., Taizhong, China. According to the GB/T528-1998 standard with a crosshead speed of 500 mm/min. The cone calorimeter tests were measured on a Fire Testing Technology cone calorimeter. The size of square specimens was 100 mm × 100 mm × 4 mm, each simple was tested twice at a heat flux of 35 kW/m^2, according to ISO 5660 standard procedures without "frame and grid". The exhaust flow was 24 L/s. The scanning electron microscopy (SEM) images of burnt samples were obtained by scanning electron microscope JEOL JSM-6360LV, Japan Electronics Co., Tokyo, Japan. Thermal stability of NR composites was performed on a Perkin-Elmer TGA 7 thermal analyzer, PerkinElmer Limited Co., Shanghai, China. The heating rate was set at 10 °C/min from room temperature to 700 °C under nitrogen with a flow rate of 80 ml/min.

2.2.6. Crosslinking density test

The crosslinking density of rubber was tested by equilibrium swelling method, and the swelling of NR was tested by n-heptane. 0.2 g sample was weighted, and its mass was signed as m_0. Then, the sample was extracted with acetone in Soxhlet extractor for 48 h, after being wrapped with filter screen. In addition, the sample was put in n-heptane to swell for 48 h at 25 °C. Then, the solvent on the sample surface was quickly removed with filter paper. Its mass was signed as m_1. Finally, the sample was dried at 50 °C. Its constant mass was signed as m_2 (drying time is about 8 h). Flory-rchner equation was used to calculate the crosslinking density, as shown in Formulas (1) and (2).

$$\mathrm{Vr} = \frac{-1}{V}\left[\frac{\ln(1-V_2)+V_2+xV_2^2}{V_2^{1/3}}\right] \quad (1)$$

$$\mathrm{V}_2 = \frac{m_2/\rho}{m_2/\rho+(m_1-m_0)\rho_s} \quad (2)$$

where Vr is the crosslinking density, mol/cm^3; x is the interaction constant of NR and n-heptane, taking 0.45; ρ is the density of NR vulcanizate, g/cm^{-1}; V is the molar volume of solvent, cm^3/mol; V_2 is the volume fraction of rubber in the sample; ρ_s is the density of solvent; m_0 is the mass of vulcanizate before swelling; m_1 is the mass of vulcanizate after swelling; m_2 is the mass of vulcanizate after drying.

3. Results and discussion

3.1. Characterization of GO-BN

After the modification of graphene oxide with boron nitride, the color of the product changed from brown-black to light brown. The chemical composition of modified graphene oxide was analyzed by XPS spectroscopy. The full XPS spectra of BN, GO, KH550-BN and GO-BN were shown in Fig. 2. In Fig. 2a, new peaks of Si2s and Si2p were observed in the all-optical spectrum of GO-BN, indicating that the sample contains new element Si, which is consistent with the FTIR results. C1s spectral fitting analysis of GO-BN (Fig. 2b) shows that there were C—C/C=C (284.6 eV), C—O (286.5 eV), O—C=O (288.9 eV), C—Si (282.6 eV) and C—N (285.6 eV) peaks (Stankovich et al., 2007). Compared with the C1s spectrum of GO (Fig. 2c), there were more C—Si and C—N peaks (Xu et al., 2015). Fig. 2d shows the N1s fitting spectrum of KH550-BN, compared with BN N1s (Fig. 2e), KH550-BN has N—C (396.7 eV) bond, which corresponds to Fig. 2b. The above data indicate that after BN was modified by KH550 and grafted with GO, Si element appeared on the surface of the sample. Furthermore, a C—N bond appeared which proofs the successful grafting of GO and BN.

The FTIR spectra of boron nitride modified graphene oxide were analyzed and are shown in Fig. 3. Comparing the a and b curves, it can be clearly seen that there are three characteristic peaks of graphene oxide at 3394 cm^{-1}, 1680 cm^{-1} and 1076 cm^{-1} corresponding to the stretching vibration peak of —OH, absorption peak of C=O stretching vibration, and C—O stretching vibration respectively. Comparing the curves of b and c, it can be observed clearly that there are obvious absorption peaks at 1380 cm^{-1} and 806 cm^{-1}, corresponding to the expansion and deformation vibration peaks of boron nitride. From the comparison between the two groups, it can be seen that there are characteristic peaks of boron nitride and graphite oxide at 1680 cm^{-1}, 1380 cm^{-1}, 1076 cm^{-1} and 806 cm^{-1} in the c curve, and the grafting process of boron nitride and graphene oxide was successfully achieved, which is consistent with the XPS results.

3.2. Thermal stability of fire retardant natural rubber

The thermal stability and char forming ability of the flame retardant nature rubber were investigated by employing the TGA technique and the corresponding data are shown in Table 2 and Fig. 4. From Fig. 4, it can be clearly seen that the initial decomposition temperature of FRNR with intumescent flame retardant is lower than that of NR. Because the decomposition temperature of the intumescent flame retardant was lower and it decomposes in advance in the early stage of combustion. The weight loss temperature of the first 10 wt% is 320 °C, which was lower than that of the pure NR about 16.9%. However, as the combustion proceeded and the flame retardants start to work, the surface area of the combustion boundary increased and an expanding carbon layer was formed. Consequently, the diffusion rate of volatile combustible debris was reduced, which leaded to the reduction of

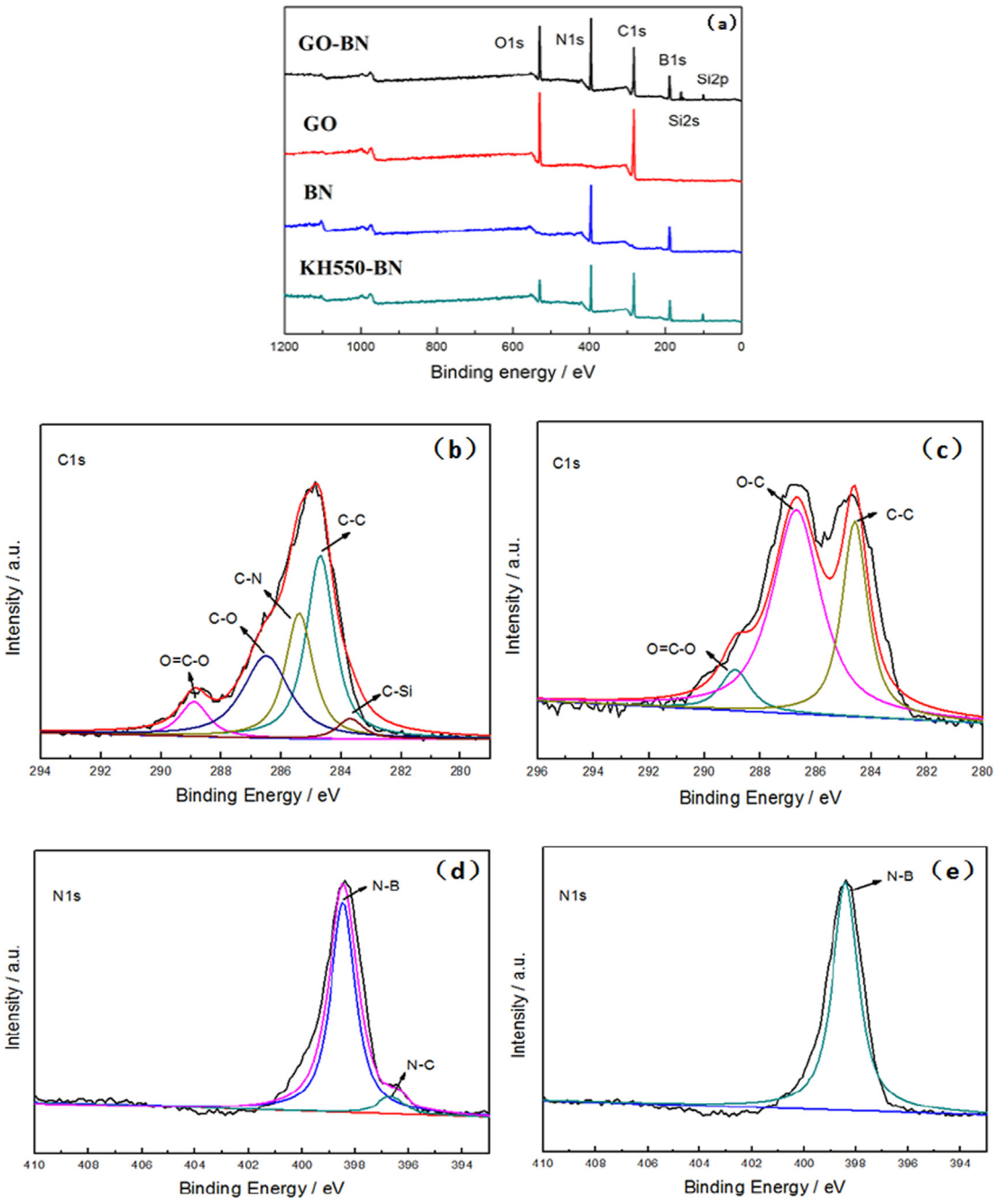

Fig. 2 XPS spectrum analysis: (a) XPS full spectrum (b) C1s spectrum of GO-BN (c) C1s spectrum of GO (d) N1s spectrum of KH550-BN (e) N1s spectrum of BN.

the mass loss rate. The sample with a content of 4 phr of GO-BN had a 34.1% char residue, and moreover, the mass loss of FRNR sample was less than that of pure sample. This improved charring was attributed to the unique layered network structure of GO-BN, which has fine thermal conductivity and carbonization performance, thus making heat transfer more uniform in the initial combustion stage. In addition, faster matrix carbonization as well as thermal decomposition of intumescent flame retardant can also occur in this same stage. When the GO-BN was increased to 12 phr, the residual carbon content of FRNR reached 38.6%. With the increase of synergist content, the carbon residue at 600 °C only increased to 39.2%. It indicated that the increase of GO-BN content increases the carbon content in the carbon layer but decreases its foaming property, therefore affecting the gas tightness of the char layer.

3.3. Intrinsic fire behavior of nature rubber

In order to evaluate the inherent flame retardancy of FRNR, the FRNR composites were evaluated by LOI and UL-94 tests. The obtained results were shown in Table 3. It can be

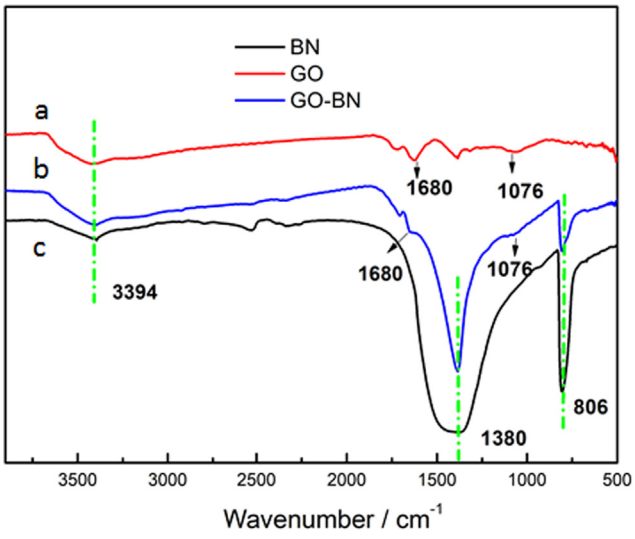

Fig. 3 Infrared Spectrum of GO-BN.

Table 2 TG data of FRNR composites.

Samples	T_{10}%/°C	W_{600}/%
NR1	385	27.9
NR2	320	33.5
NR3	325	34.1
NR4	309	33.6
NR5	369	38.6
NR6	376	39.2

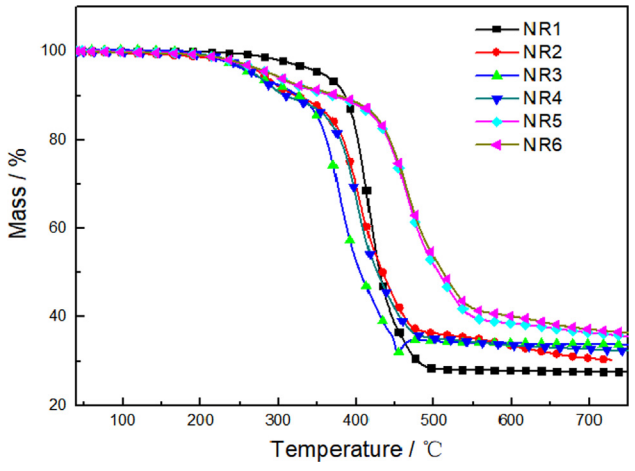

Fig. 4 TG curves of natural rubber (NR) and FRNR composites.

seen from Table 3, that NR was highly flammable. During the experiment, a strong flame was observed accompanied by smoke. Its LOI value was measured and found to be 18.2%, and it did not reach any rating in the UL-94 test. When IFR was added to natural rubber, the LOI value of NR2 increased rapidly, and the flame retardancy of NR2 increased greatly,

Table 3 LOI and UL-94 of FRNR Composites.

Samples	LOI (%)	UL-94
NR1	18.2	No Rating
NR2	24.1	V-1
NR3	25.5	V-1
NR4	25.8	V-1
NR5	25.9	V-0
NR6	26.1	V-0

reaching an LOI value of 24.1% and a vertical combustion test grade reaches V-1. Because the IFR can promote the formation of a thick porous char layer on the substrate and cover the polymer combustion surface. This carbon layer can effectively block the exchange of external heat and combustion gas in the combustion area, dilute the oxygen concentration in the combustion area, reduce the temperature in the combustion zone, and play a role in suppressing combustion, which results in the increased the LOI value of the sample. Moreover, with the addition of 4 phr of flame retardant synergist GO-BN, it was found that the LOI of NR3 increased to 25.5%, which was higher than that of NR2. This improvement is attributed to the GO-BN lamellar structure and its good thermal stability. This structure is difficult to decompose in combustion process, and can strengthen the carbon layer during the combustion process. Furthermore, when the GO-BN content was increased, it was found that the LOI value of NR6 reaches to 26.1% and the vertical combustion grade reaches V-0. It clearly demonstrates that the flame retardancy of the system can be improved with the increased synergist content. However, comparing NR6 with NR5, it was found that the LOI value of NR6 only increased by 0.02%. This indicated that adding appropriate GO-BN would promote the formation of the carbon layer, thus improving the thermal stability. While adding excessive amounts of GO-BN had little effect on it.

In order to further study the flame retardant and fire safety properties of FRNR, a cone calorimetry test was carried out. The cone test is a bench scale fire test that can simulate the actual combustion of the material in the real fire conditions. The test data obtained from the test can give information on the combustion behavior of the material in fire. The results of the cone calorimeter test are presented in Fig. 5 and Table 4, the natural rubber burned rapidly and releases heat in 14 s. Meanwhile, the first HRR peak appears. As the combustion proceeds, the PHRR first decreases and then rised, and then a second peak appeard. This is because on heating the rubber component, its surface was cross-linked and carbonized and the carbon layers blocked oxygen and heat transfer from outside. At this time, combustion was suppressed and the first peak appeared. However, as the combustion depth increased, the surface carbon layer was destroyed. Moreover, the rubber under the carbon layers continued to crack, releasing more combustible gas, while the total heat release (THR) and HRR reached the maximum value. Compared with pure NR without IFR, the PHRR and THR of NR2 decreased by 28% and 3%. This improvement is attributed to the char layers formed by IFR, which can block the exchange of oxygen and heat from inside and outside. The IFR had a low decomposition temperature and poor thermal stability, and could decompose at 200 °C. PER can produce ester polyols and the acid as a dehydrating agent. Ester polyols carbonized those

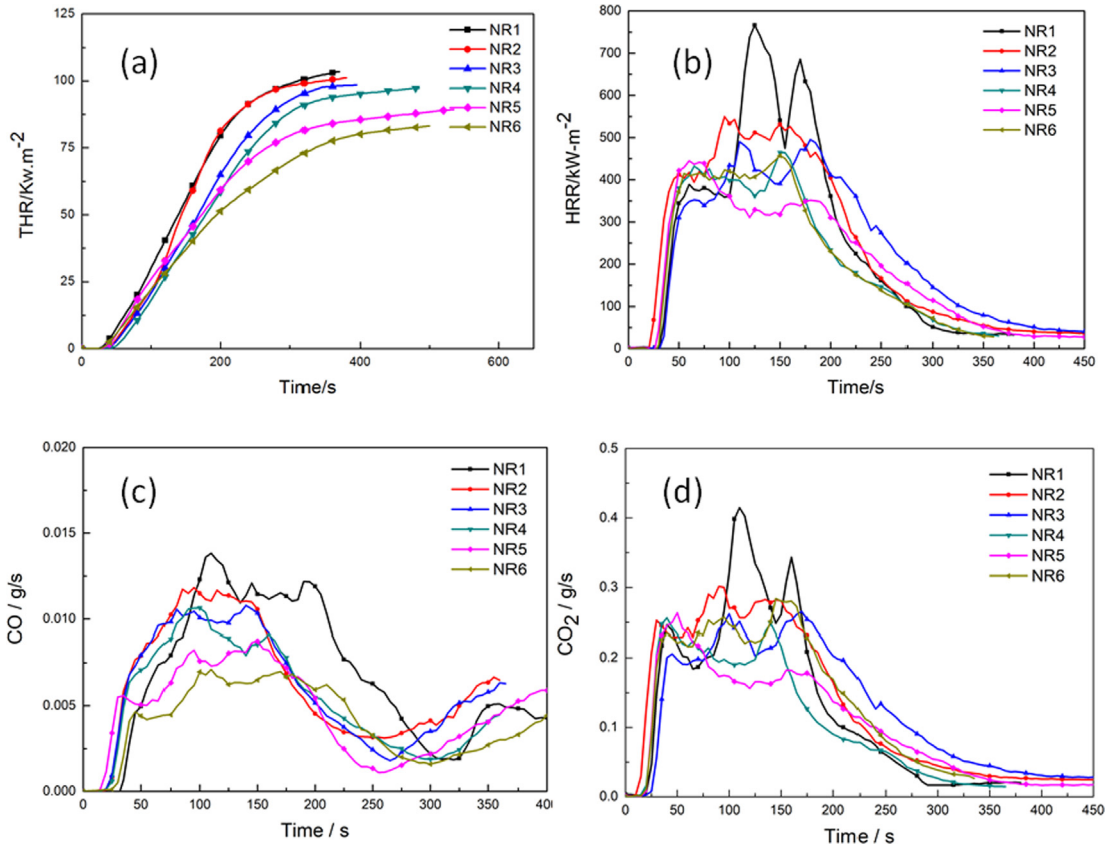

Fig. 5 (a) HRR curves of the Nature Rubber (NR) and FR-NR; (b) THR curves of the Nature Rubber (NR) and FR-NR; (c) CO curves of the Nature Rubber (NR) and FR-NR; (d) CO2 curves of the Nature Rubber (NR) and FR-NR.

Table 4 Cone calorimetry data for the NR and FRNR.

Samples	PHRR (kW/m^2)	THR (MJ/m^2)	Time to Ignition (s)	FRI
NR1	766	103	14	1
NR2	551	100	15	1.53
NR3	492	98	18	2.10
NR4	456	96	19	2.45
NR5	438	83	20	3.10
NR6	458	79	22	3.42

produced molecules of water to decrease the temperature of environment and the acid had an esterification reaction with PER to form carbon layers. MEL and APP can also produce non-combustible gas NH_3 and H_2O, which expanded the carbon layers. This combined phenomenon enables the IFR to possess high flame retardancy efficiency. Furthermore, with the addition of GO-BN, all FRNRs containing synergists further had decreased PHRR compared to the pure samples, indicating that GO-BN and IFR had synergistic effects (Wu et al., 2019). Additionally, the ignition time was further prolonged, because the addition of GO-BN affect the heat transfer of the system, it maked the heat transfer more uniform, and avoided local high heat caused by non-uniform heat transfer (Tu et al., 2019; Kisang et al., 2015; Zhang et al., 2018). It can also be seen from Fig. 5 that the sample NR5 with 12 phr content of GO-BN showed an improved flame retardancy. The combustion time of FRNR was extended to 20 s. PHRR and THR were reduced by 43% and 20% respectively. The decrease of the PHRR and THR of NR5 composites was attributed to the good thermal conductivity of GO-BN. The peak heat release rate curve of NR5 sample became smoother compared to that of natural rubber, indicating that GO-BN synergistic IFR will form a new carbon layer after the initial carbon layer was destroyed during combustion, accompanied by a virtuous cycle of carbon layer destruction until the end of combustion. From the THR curve and CO and CO_2 release curve, it can be seen that the addition of GO-BN flame retardant was inversely proportional to the total heat release, CO and CO_2 release, which showd that GO-BN flame retardant can control the combustion behavior of the system well and has good flame retardancy.

FRI is a kind of intuitionistic expression of the excellent degree of flame retardancy performance of materials (Vahabi et al., 2019). The results of cone calorimetry are summarized.

The FRI of FRNR is calculated by PHRR; THR and TTI. It was found that the FRI value of NR2 with IFR only was 1.53, which was less than that with GO-BN, indicating that the addition of GO-BN improved the flame retardancy of FRNR. With the increase of GO-BN, the FRI value also increased. When the amount of GO-BN was 16 phr, the FRI value was the highest, which is 3.42. It showed that NR6 had good flame retardancy. The above results showed that GO-BN had a good synergistic effect of flame retardant.

3.4. Morphology of burnt composites

It is well known that a continuous and compact carbon layer can be regarded as a good insulation barrier to insulate heat and oxygen. Scanning electron microscopy (SEM) was employed to analyze the structure and morphology of the residual carbon from the LOI test, as shown in Fig. 6. It can be seen from Fig. 6a that the coke structure formed by burning pure NR1 had cracks and defects. This was because NR does not form an effective protective carbon layer on its surface during the combustion process, resulting in the combustion part of the substrate and external heat and combustible gas exchanged, which leaded to no obvious flame retardant effect. The SEM images of NR2 combustion residues with intumescent flame retardants showed the formation of a complete carbon layer with large amount of bubbles after full combustion of the system had a large number of bubbles. This was due to the thermal decomposition of the gas source in the intumescent flame retardant into the nonflammable gases H_2O and CO_2, and the acid source catalyzes the formation of carbon. The carbon layer expanded obviously, the surface of the carbon layer had folds and protrusions, and the strength of the carbon layer increased, which maked the carbon layer easier to maintain at high-temperature conditions. However, the NR3, NR4, NR5, and NR6 samples with different GO-BN content were found to be different from that of the intumescent flame retardant. The SEM image showed that the system formed a relatively compact carbon layer on the surface

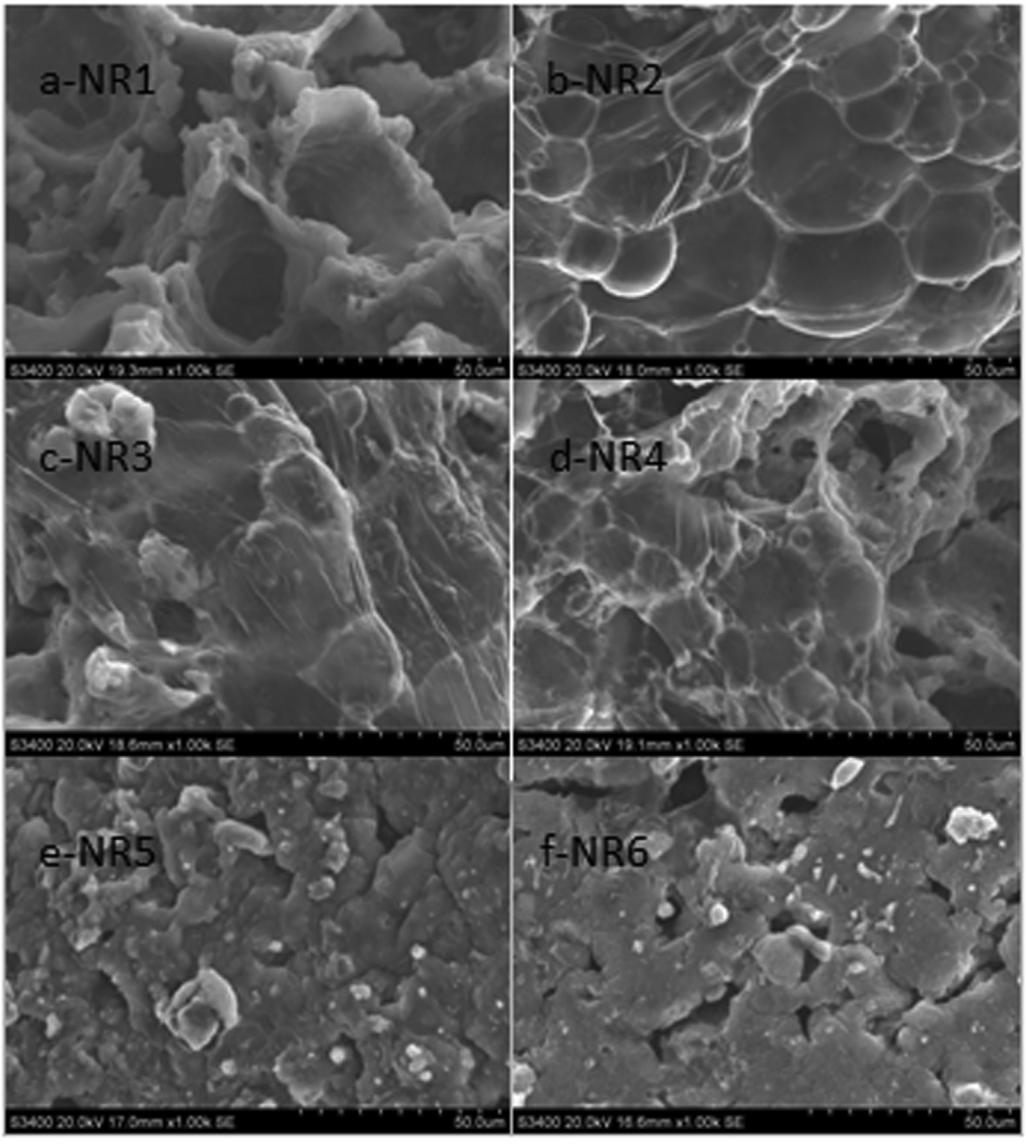

Fig. 6 SEM Images of Residual Carbon in FRNR.

after combustion. Moreover, with subsequent increase of GO-BN content in the system, the foamed carbon layer gradually decreased while the pores on the carbon layer increased gradually. Although the carbon content in the carbon layer increased with the increase of GO-BN content, it was observed that excessive GO-BN reduces the foaming properties of the carbon layer, thus affecting the gas tightness of the carbon layer.

In order to study the flame retardant mechanism of natural rubber (NR) and the synergistic effect of the interaction between IFR and GO-BN, the residual carbon produced after combustion in muffle furnace was analyzed by FTIR. It can be seen from Fig. 7 that all combustion products have an absorption peak at 3430 cm^{-1}, indicating that some hydroxyl groups (—OH) containing compounds were produced during combustion. All six samples showed vibration absorption peaks of the aromatic fused ring skeleton at 1626 cm^{-1}, and this structure can effectively improve the thermal stability of the FRNR. However, in contrast to the NR1 sample without synergist, the FRNR with other synergists, specifically NR2, NR3, NR4, NR5 and NR6, showed peaks at 1305 cm^{-1} and 992 cm^{-1} which corresponded to the P═O and P—O bonds of polyphosphoric acid produced by APP decomposition in IFR. Continuous observation showed that the peak of NR5 at 992 cm^{-1} was significantly enhanced, suggesting that an optimal amount of the synergist was added. However, with the increase of GO-BN, it was found that the peak depth of NR6 at 992 cm^{-1} decreased dramatically, because too much GO-BN could inhibit the decomposition of APP, and the foaming properties of carbon layer decreased. In addition, there are C═O bond absorption peaks and methyl tensile vibration peaks at 779 cm^{-1} and 1382 cm^{-1}. The above peaks indicate that the residual carbon of the flame retardant rubber system after combustion was a mixture of small water molecules, NH_3, phosphorus, oxygen, nitrogen-containing compounds, aromatic compounds and silicon oxide. It can also be seen that the thermal decomposition of rubber molecular chains forms aromatic structures with high stability. The P═O bond in char residue is attributed to polyphosphoric acid, which was a product of the thermal decomposition of ammonium polyphosphate in the intumescent flame retardant,

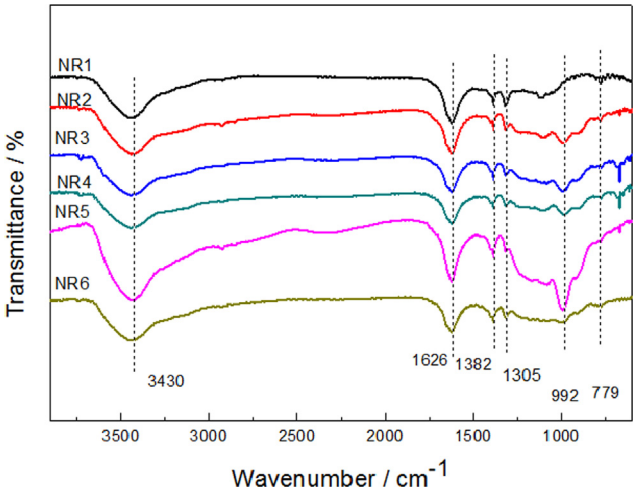

Fig. 7 FTIR Spectra of Residual Carbon of FRNR.

Table 5 Mechanical properties of FRNR Composites.

Samples	Tensile Strength/ MPa	Elongation at Break/%	Crosslinking density/ 10^{-3}mol·cm^{-3}
NR1	26.2	521	3.26
NR2	8.8	314	2.58
NR3	16.9	344	2.99
NR4	13.8	328	2.84
NR5	10.6	317	2.79
NR6	9.6	272	2.71

which can effectively improve the barrier ability of carbon layer.

3.5. Mechanical properties

The mechanical properties of FRNR composites are listed in Table 5. The tensile strength and elongation at break of NR were 26.2 MPa and 521.4%, whereas they were 8.8 MPa and 314.5% for NR/IFR composites, respectively. It was found that the IFR remarkably decrease its mechanical properties. The great difference in polarity between the NR matrix and IFR fillers led to incompatibility and poor dispersion. In contrast, when GO-BN was used as flame retardant synergist, the tensile strength and elongation at break were improved. This is due to the addition of synergistic agent GO-BN, which has a high specific surface area and improves the migration resistance of flame retardant in natural rubber. The agglomerated flame retardants become broken, which reduces the amount of agglomerates in FRNR. The flame retardant can be dispersed better in natural rubber, thus increasing the crosslinking sites and increasing the adhesive density of rubber. When the cross-linking density reaches a certain degree, a good mechanical network can be formed in the rubber system, which increases the mechanical properties of the composites. However, when the amount of the flame retardant synergist GO-BN is added in excess, the mechanical properties of rubber decrease relatively. This result confirmed that the GO-BN can improve not only flame retardant properties but also mechanical performance.

4. Conclusions

In this work, we have successfully synthesized a new flame retardant synergist GO-BN and applied it with an intumescent flame retardant in natural rubber. FTIR and XPS tests confirmed the successful synthesis of GO-BN. Moreover, the flame retardancy of FRNR was studied by LOI, UL-94, cone calorimetry and TG tests. Remarkably, when 12 phr of flame retardant GO-BN was added, a maximum limit oxygen index (LOI) of 25.9% was recorded, which was 42% higher than that of pure natural rubber. The cone calorimetry results, showed that with 12 phr of flame retardant GO-BN, the HRR decreased to 438 KW/m^2, while the THR decreased to 83 MJ/m^2, corresponding to a decrease of 42.5% and 23.3% compared to natural rubber. Furthermore, a similar phenomenon was observed in the amount of CO and CO_2 produced. Among the composites, the sample with 12 phr content of GO-BN showed the best flame retardancy perfor-

mance with a residual carbon of 38.56% at 600 °C. These results show that GO-BN and intumescent flame retardant have a good synergistic effect on the thermal stability and charring properties of natural rubber, and are easy to form a dense carbon layer structure with high temperature and oxygen transfer resistance.

Funding

Na Wang gratefully acknowledges the financial support for her research group by the National Natural Science Foundation of China (Grant No. [51973124]); National Key R&D Program "Science and Technology Winter Olympics" (Grant No. 2019YFF0302004); Sino-Spanish Advanced Materials Institute, Shenyang Municipal Science and Technology Bureau (Grant No. 18-005-6-04); Department of Science & Technology of Liaoning province-Shenyang National Laboratory for Materials Science Joint R & D Fund Project (Grant No. 2019JH3/30100015); Liaoning BaiQianWan Talents Program (Grant No. [2020]78).

References

Alongi, J., Han, Z.D., Bourbigot, S., 2015. Intumescence: tradition versus novelty. A comprehensive review. Prog. Polym. Sci. 51, 28–73.

Carli, L.N., Roncato, C.R., Zanchet, A., Mauler, R.S., Giovanela, M., Brandalise, R.N., Crespo, J.S., 2011. Characterization of natural rubber nanocomposites filled with organoclay as a substitute for silica obtained by the conventional two-roll mill method. Appl. Clay Sci. 52, 56–61.

Chen, S.B., Li, T.X., Wan, S.H., Huang, X., Cai, S.W., He, X.R., Zhang, R., 2019. Effect of nitrogen-doped graphene oxide on the aging behavior of nitrile-butadiene rubber. Polymers 11, 1637–1651.

Cui, Z., Qu, B.J., 2010. Synergistic effects of layered double hydroxide with phosphorus-nitrogen intumescent flame retardant in PP/EPDM/IFR/LDH nanocomposites. Chin. J. Polym. Sci. 4, 563–571.

Das, M., Ghatak, S., 2012. Synthesis of boron nitrides from boron containing poly(vinylalcohol) as ceramic precursory. Bull. Mater. Sci. 35, 99–102.

Das, M., Ghosh, J., Basu, A.K., 2010. Effect of activation on boron nitride coating on carbon fiber. Ceram. Int. 36, 2511–2514.

Fan, Z.C., Sun, L.X., Wu, S.N., Liu, C., Wang, M.J., Xu, J.S., Zhang, X.B., Tong, Z.W., 2019. Preparation of manganese porphyrin/niobium tungstate nanocomposites for enhanced electrochemical detection of nitrite. J. Mater. Sci. 54, 10204–10216.

Fang, S., Hu, Y., Song, L., Zhan, J., He, Q., 2008. Mechanical properties, fire performance and thermal stability of magnesium hydroxide sulfate hydrate whiskers flame retardant silicone rubber. J. Mater. Sci. 43, 1057–1062.

Feng, Y.Z., Li, X.W., Zhao, X.Y., Ye, Y.S., Zhou, X.P., Liu, H., Liu, C.T., Xie, X.L., 2018. Synergetic improvement in thermal conductivity and flame retardancy of epoxy/silver nanowires composites by incorporating "branch-like" flame-retardant functionalized graphene. ACS Appl. Mater. Interfaces 10, 21628–21641.

Feng, Y.Z., Wang, B., Li, X.W., Ye, Y.S., Ma, J.M., Liu, C.T., Zhou, X.P., Xie, X.L., 2019. Enhancing thermal oxidation and fire resistance of reduced graphene oxide by phosphorus and nitrogen co-doping: mechanism and kinetic analysis. Carbon 146, 650–659.

Feng, Y.Z., Han, G.J., Wang, B., Zhou, X.P., Ma, J.M., Ye, Y.S., Liu, C.T., Xie, X.L., 2020. Multiple synergistic effects of graphene-based hybrid and hexagonal born nitride in enhancing thermal conductivity and flame retardancy of epoxy. Chem. Eng. J. 379, 122402.

Guo, Y.Q., Bao, C.L., Song, L., Yuan, B.H., Hu, Y., 2011. In situ polymerization of grapheme graphite oxide and functionalized graphite oxide into epoxy resin and comparison study of on-the-flame behavior. Ind. Eng. Chem. Res. 50, 7772–7783.

Iqbal, S.S., Inam, F., Iqbal, N., Jamil, T., Bashir, A., Shahid, M., 2016. Thermogravimetric, differential scanning calorimetric, and experimental thermal transport study of functionalized nanokaolinite-doped elastomeric nanocomposites. J. Therm. Anal. Calorim. 125, 871–880.

Kahraman, G., Wang, D.Y., Jonas, V.I., Gallei, M., Evamarie, H.H., Eren, T., 2019. Synthesis and characterization of phosphorus- and carborane-containing polyoxanorbornene block copolymers. Polymers 11, 613–629.

Kisang, A., Kiho, K., Myeongjin, K., Jooheon, K., 2015. Fabrication of silicon carbonitride-covered boron nitride/nylon 6,6 composite for enhanced thermal conductivity by melt process. Ceram. Int. 41, 2187–2195.

Qin, Z.L., Li, D.H., Yang, R.J., 2016. Effect of nano-aluminum hydroxide on mechanical properties, flame retardancy and combustion behavior of intumescent flame retarded polypropylene. Mater. Des. 89, 988–995.

Qiu, S.L., Hu, W.Z., Yu, B., Yuan, B.H., Zhu, Y.L., Jiang, S.H., Wang, B.B., Song, L., 2015. Effect of functionalized graphene oxide with organophosphorus oligomer on the thermal and mechanical properties and fire safety of polystyrene. Ind. Eng. Chem. Res. 54, 3309–3319.

Rabe, S.Y., Chuenban, B., 2017. Schartel, Exploring the modes of action of phosphorus-based flame retardants in polymeric systems. Materials. 10, 445–468.

Rabe, S., Chuenban, Y., Schartel, B., 2017. Exploring the modes of action of phosphorus-based flame retardants inpolymeric systems. Materials. 10, 445–468.

Sasan, M., Yolanda, C., Frida, R., John, M.H., 2019. Achieving high thermal conductivity in epoxy composites: effect of boron nitride particle size and matrix-filler interface. Polymers 11, 1156–1173.

Stankovich, S., Dikin, D.A., Piner, R.D., Kohlhaas, K.A., Kleinhammes, A., Jia, Y., Wu, Y., Nguyen, S.T., Ruoff, R.S., 2007. Synthesis of graphene-based nanosheets via chemical reduction of exfoliated graphite oxide. Carbon 45, 1558–1565.

Stengl, V., Henych, J., Kormunda, M., 2014. Self-Assembled BN and BCN quantum dots obtained from high intensity ultrasound exfoliated nanosheets. Sci. Adv. Mater. 6, 1106–1116.

Tang, Y., Hu, Y., Wang, S., Gui, Z., Fan, W., 2003. Intumescent flame retardant–montmorillonite synergism in polypropylene-ayered silicate nanocomposites. Polym. Int. 52, 1396–1400.

Tu, L., Xiao, Q., Wei, R.B., Liu, X.B., 2019. Fabrication and enhanced thermal conductivity of boron nitride and polyarylene ether nitrile hybrids. Polymers 11, 1340–1355.

Vahabi, H., Jouyandeh, M., Cochez, M., Khalili, R., Vagner, C., Ferriol, M., Movahedifar, E., Ramezanzadeh, B., Rostami, M., Ranjba, Z., Hadavand, B.S., Saeb, M.R., 2018. Short-lasting fire in partially and completely cured epoxy coatings containing expandable graphite and halloysite nanotube additives. Prog. Org. Coat. 123, 160–167.

Vahabi, H., Saeb, M.R., Formela, K., Cuesta, J.M.L., 2018. Flame retardant epoxy/halloysite nanotubes nanocomposite coatings: exploring low-concentration threshold for flammability compared to expandable graphite as superior fire retardant. Prog. Org. Coat. 119, 8–14.

Vahabi, H., Kandola, B.K., Saeb, M.R., 2019. Flame retardancy index for thermoplastic composites. Polymers 11, 407.

Wang, J.C., Dong, X.Y., Hao, W.L., Zhao, Y., Guo, X., Wu, d., 2013. Application properties of TCP/OMMT flame-retardant system in NR composites. J. Elastomers Plast. 45, 107–119.

Wang, N., Mi, L., Wu, Y.H., Zhang, J., Fang, Q.H., 2014. Double-layered co-microencapsulated ammonium polyphosphate and

mesoporous MCM-41 in intumescent flame-retardant natural rubber composites. J. Therm. Anal. Calorim. 115, 1173–1181.
Wang, N., Xu, G., Wu, Y.H., Zhang, J., Hu, L.D., Luan, H.H., Fang, Q.H., 2016. The influence of expandable graphite on double-layered microcapsules in intumescent flame-retardant natural rubber composites. J. Therm. Anal. Calorim. 12, 1239–1251.
Wang, N., Xu, G., Wu, Y.H., Zhang, J., Hu, L.D., Luan, H.H., Fang, Q.H., 2016. The influence of expandable graphite on double-layered microcapsules in intumescent flame-retardant natural rubber composites. J. Therm. Anal. Calorim. 123, 1239–1251.
Wang, N., Hu, L.D., Babu, H.V., Zhang, J., Fang, Q.H., 2017. Effect of tea saponin-based intumescent flame retardant on thermal stability, mechanical property and flame retardancy of natural rubber composites. J. Therm. Anal. Calorim. 128, 1133–1142.
Wang, N., Wang, S.W., Chen, J.S., Wang, S., 2018. Journal of benzoic acid functionalized graphene-Al(OH)3 synergistic flame retardant polypropylene. Composites 35, 2434–2441.
Wang, Chao, Wu, Yicheng, Li, Yingchun, Shao, Qian, Yan, Xingru, Han, Cui, Wang, Zhe, Liu, Zhen, Guo, Zhanhu, 2018. Flame-retardant rigid polyurethane foam with a phosphorus-nitrogen single intumescent flame retardant. Polym. Adv. Technol. 29 (1), 668–676. https://doi.org/10.1002/pat.v29.110.1002/pat.4105.
Wang, J.C., Yang, K., Zheng, X.Y., 2009. Studies on the effect of 4A zeolite on the properties of intumescent flame-retardant agent filled natural rubber composites. J. Polym. Res. 16, 427–436.
Wang, N., Zhang, M., Kang, P., Zhang, J., Fang, Q.H., Li, W.D., 2018. Synergistic effect of graphene oxide and mesoporous structure on flame retardancy of nature rubber/IFR composites. Materials 11, 1005–1018.
Wu, C., Wang, X.D., Zhang, J.Y., Cheng, J., Shi, L., 2019. Microencapsulation and surface functionalization of ammonium polyphosphate via insitu polymerization and thiol-ene photograted reaction for application in flame-retardant natural rubber. Ind. Eng. Chem. Res. 58, 17346–17358.
Xu, M.L., Chen, Y.J., Qian, L.J., Wang, J.Y., Tang, S., 2015. Component ratio effects of hyperbranched triazine compound and ammonium polyphosphate in flame-retardant polypropylene composites. J. Appl. Polym. Sci. 131, 179–180.
Xue, Z.X., Zhang, W.W., Yan, M., Liu, J.J., Wang, B.B., Xia, Y.Z., 2017. Pyrolysis products and thermal degradation mechanism of intrinsically flame-retardant carrageenan fiber. RSC Adv. 7, 25253–25264.
Yan, W., Zhang, M.Q., Yu, J., Nie, S.H., Zhang, D.Q., Qin, S.H., 2019. Synergistic flame-retardant effect of epoxy resin combined with phenethyl-bridged DOPO derivative and graphene nanosheets. Chin. J. Polym. Sci. 37, 79–88.
Yang, H., Yang, C.Q., 2005. Durable flame retardant finishing of the nylon/cotton blend fabric using a hydroxyl-functional organophosphorus oligomer. Polym. Degrad. Stab. 88, 363–370.
Yu, B., Shi, Y.Q., Yuan, B.H., Qiu, S.L., Xing, W.Y., Hu, W.Z., Song, L., Lo, S.M., Hu, Y., 2015. Enhanced thermal and flame retardant properties of flame-retardant-wrapped graphene/epoxy resin nanocomposites. J. Mater. Chem. A 15, 8034–8044.
Zhang, J., Chen, N., Su, P., Li, M., Feng, C., 2017. Fluoride removal from aqueous solution by zirconium-chitosan/graphene oxide membrane. React. Funct. Polym. 114, 127–135.
Zhang, G.D., Fan, L., Bai, L., He, M.H., Zhai, L., Mo, S., 2018. Mesoscopic simulation assistant design of immiscible polyimide/BN blend films with enhanced thermal conductivity Chinese. J. Polym. Sci. 12, 1394–1402.
Zhoong, B., Zhang, T., Huang, X.X., Wen, G.W., Chen, J.W., Wang, C.J., Huang, Y.D., 2015. Fabrication and Raman scattering behavior of novel turbostatic BN thin films. Mater. Lett. 151, 130–133.